RESERVOIR CHARACTERIZATION AND CAPACITY CALCULATION FOR CO_2 STORAGE USING AI/ML TECHNIQUES IN GANDHAR OIL FIELD, CAMBAY BASIN, INDIA

By

Akash Nair

Under the guidance of

Prof. William K. Mohanty

Professor, IIT Kharagpur, India

Dr. Srikumar Roy

Senior Research Scientist, iCRAG,
University College Dublin, Ireland

Capacity Calculation for CO_2 Storage

$$M_{CO_2} = \rho_{CO_2res}\left[R_f \times A \times h \times \phi \times (1 - S_w) - V_{iw} + V_{pw}\right]$$

ρ_{CO_2res} is the density of CO2 at reservoir conditions

R_f is the recovery factor

A is the area of the field,

h is the effective thickness of the reservoir

ϕ is the porosity,

S_w is the water saturation,

V_{iw} is the volume of injected water
V_{pw} is the volume of produced water.

$$\mathrm{M}_{\mathrm{CO_2eff}} = 0.5 \times \mathrm{M}_{\mathrm{CO_2res}}$$

Objectives

❖ CO_2 Storage Capacity of Gandhar Oilfield

- **Properties to be found using Conventional RC and AI/ML**
  - Pay zone thickness
  - Oil Saturation
  - Porosity

- **Algorithms to be tested:**
  - Naive Bayes
  - Logistic Regression
  - Decision Tree
  - Support Vector Machine
  - Kernel Support Vector Machine
  - XGBoost
  - Random Forest
  - K-Nearest Neighbors
  - Artificial Neural Network

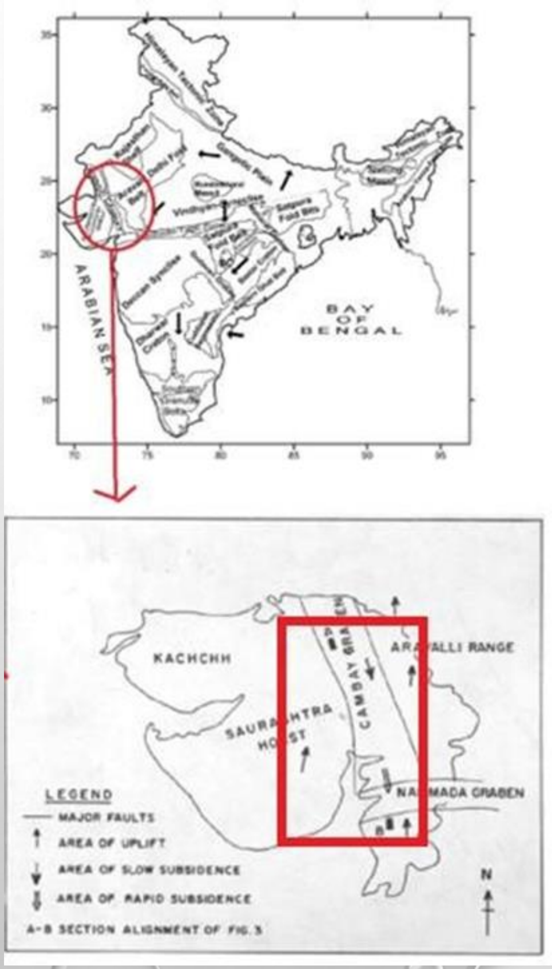

Data Used

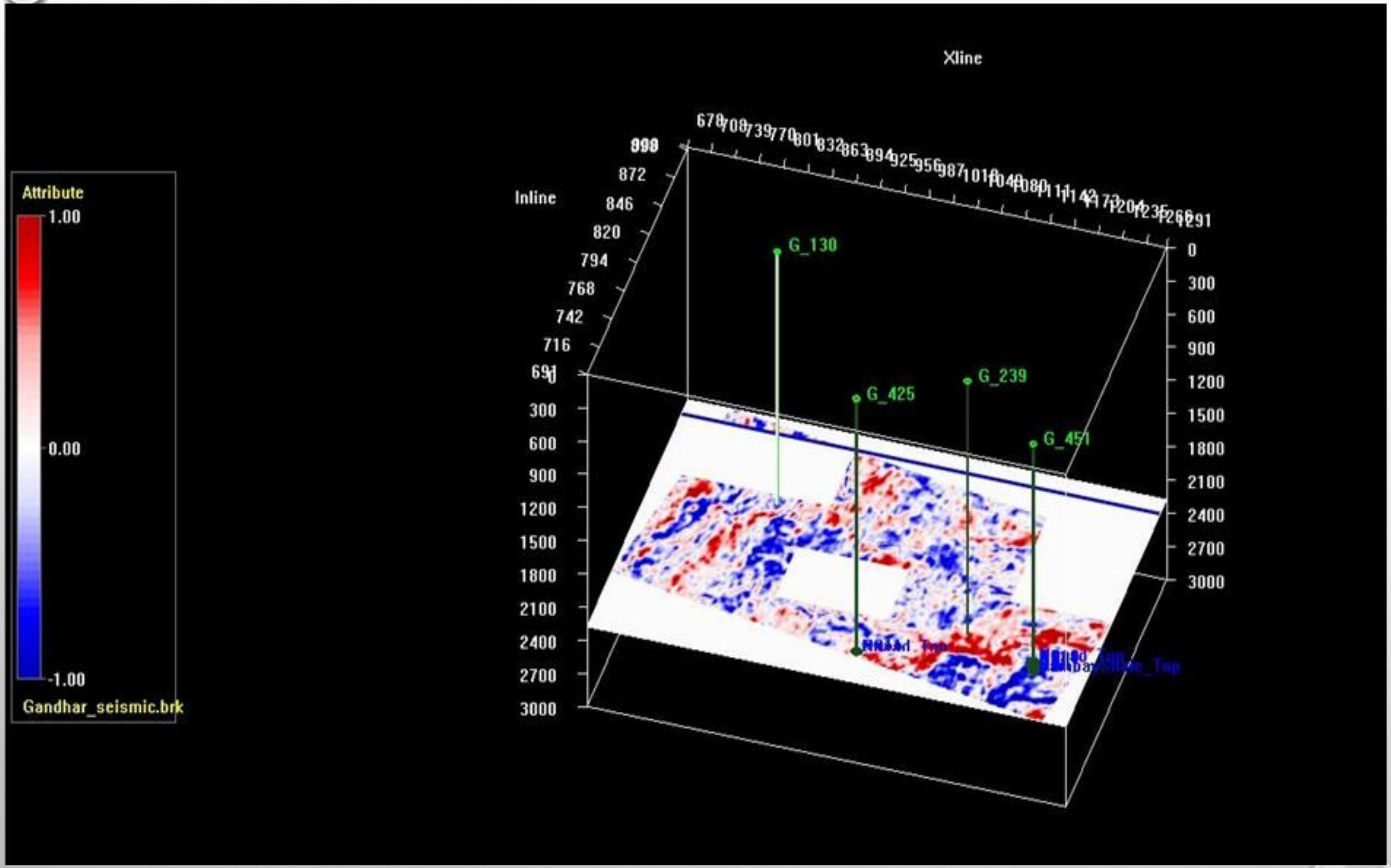

Seismic
- TWT section
- Envelope
- Instantaneous Frequency
- Impedance
- Sweetness

Well-logs
- Resistivity
- Gamma Ray
- Self-Potential
- P-wave velocity
- Porosity

Methodology

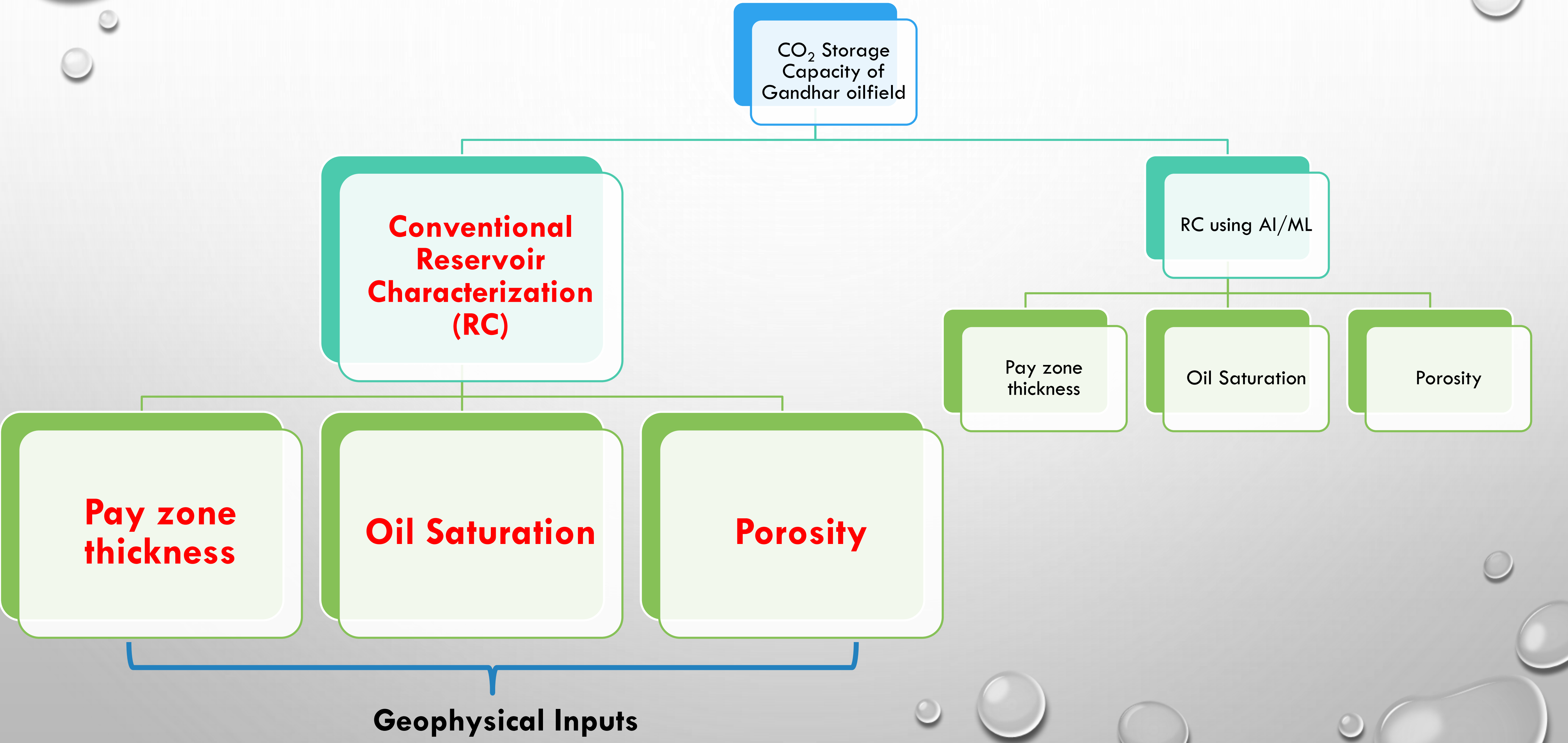

Conventional Reservoir Characterization

Seismic-to-well tie → RC using well data → RC using seismic data

RC using well data

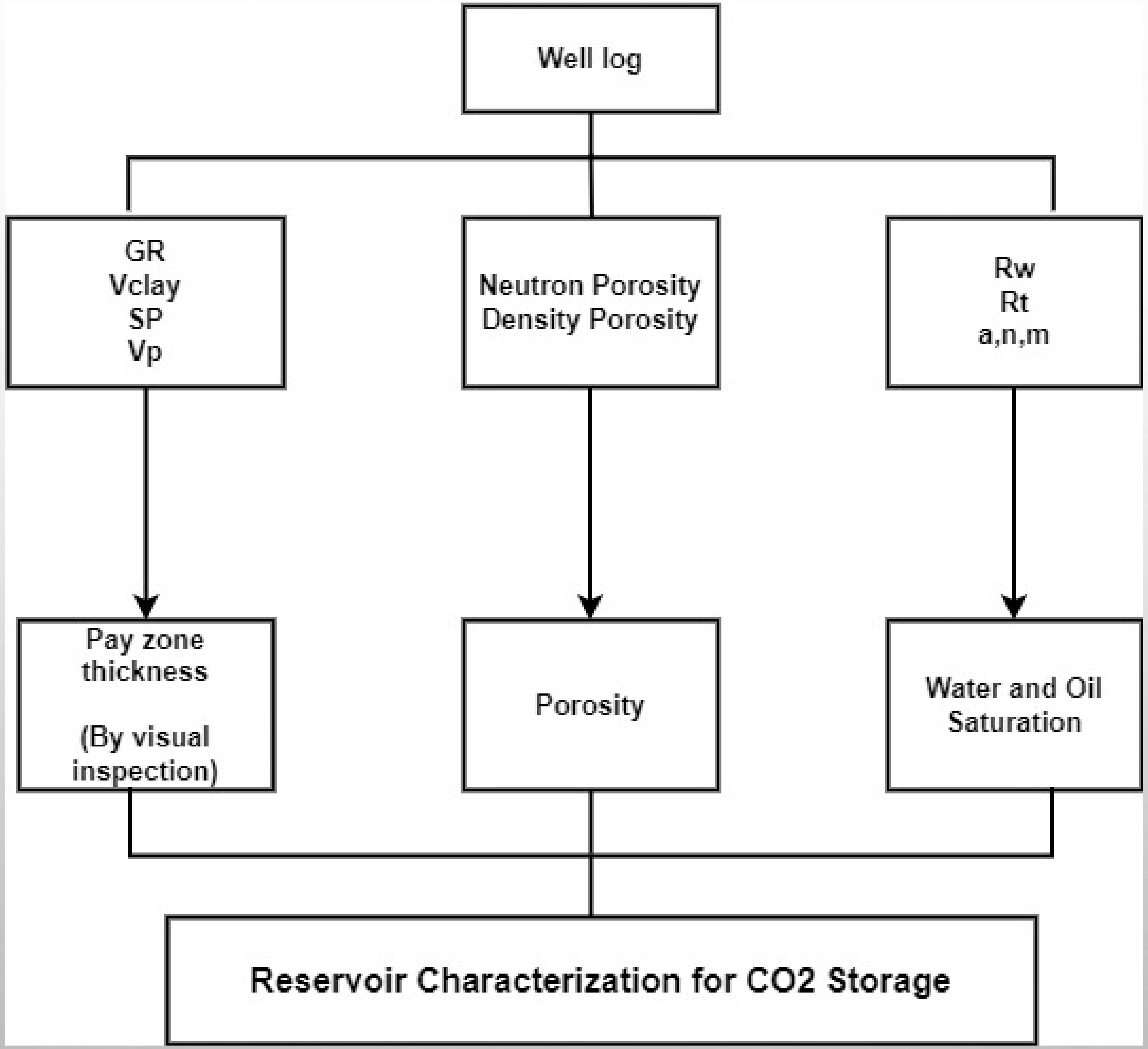

RESULTS

CONVENTIONAL RESERVOIR CHARACTERIZATION

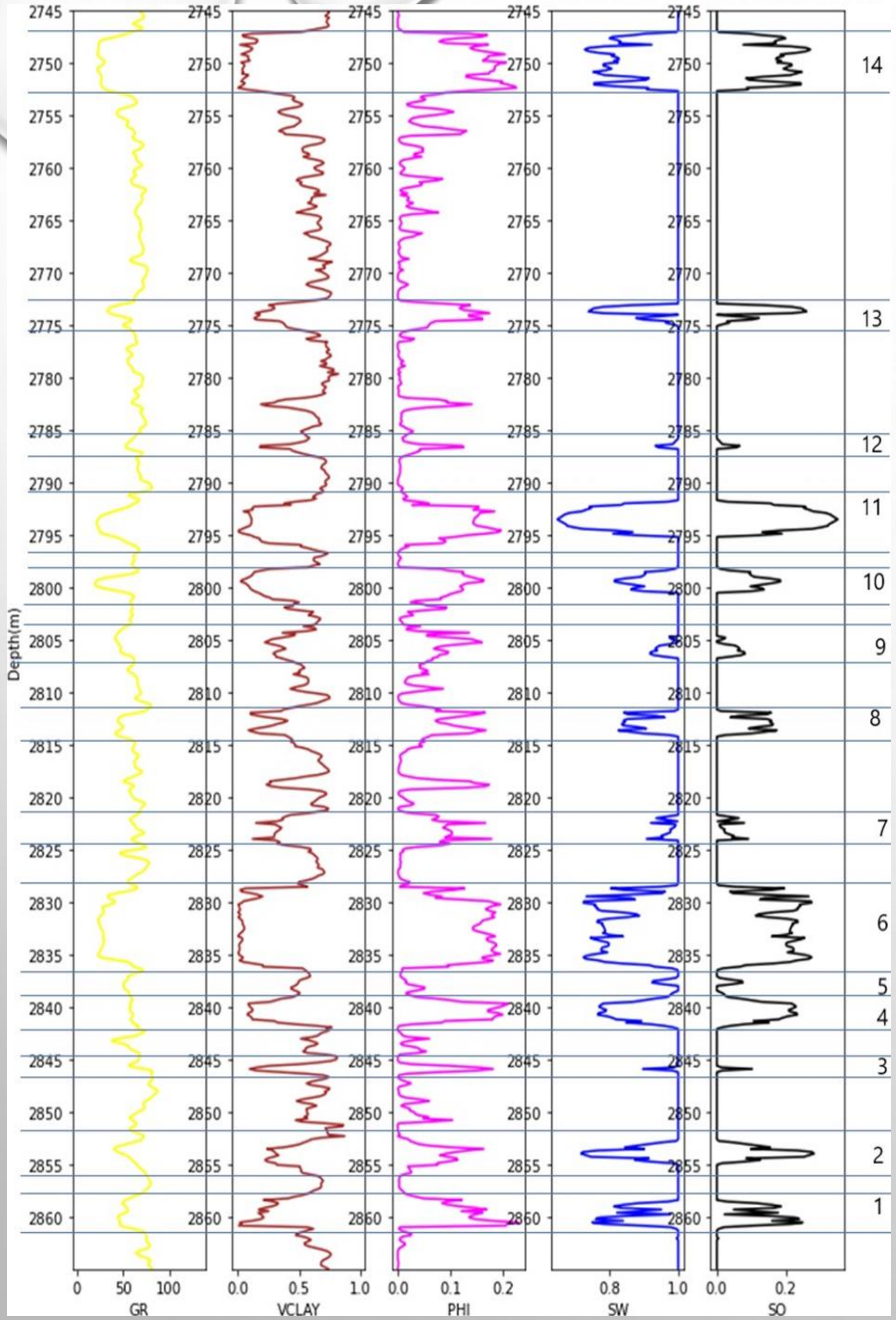

Pay Zone	Depth (m)	Thickness (m)	Porosity (%)	Oil Saturation (%)	Water Saturation (%)
14	2747-2753	6	16.45	18.25	81.75
13	2773-2776	3	13.63	14.85	85.15
12	2786-2787	1	12.46	6.16	93.84
11	2791-2795	4	14.28	25.45	74.55
10	2798-2801	3	13.05	12.2	87.8
9	2804-2807	3	8.36	6.37	93.63
8	2811-2814	3	12.22	12.91	87.09
7	2821-2825	4	10.03	3.49	96.51
6	2829-2836.5	7.5	15.67	19.93	80.07
5	2837-2838	1	1.64	5.68	94.32
4	2839-2842	3	13.78	16.08	83.92
3	2845-2847	2	18.18	10.25	89.75
2	2853-2855	2	9.98	17.14	82.86
1	2858-2861	3	14.93	14.74	85.26

Methodology

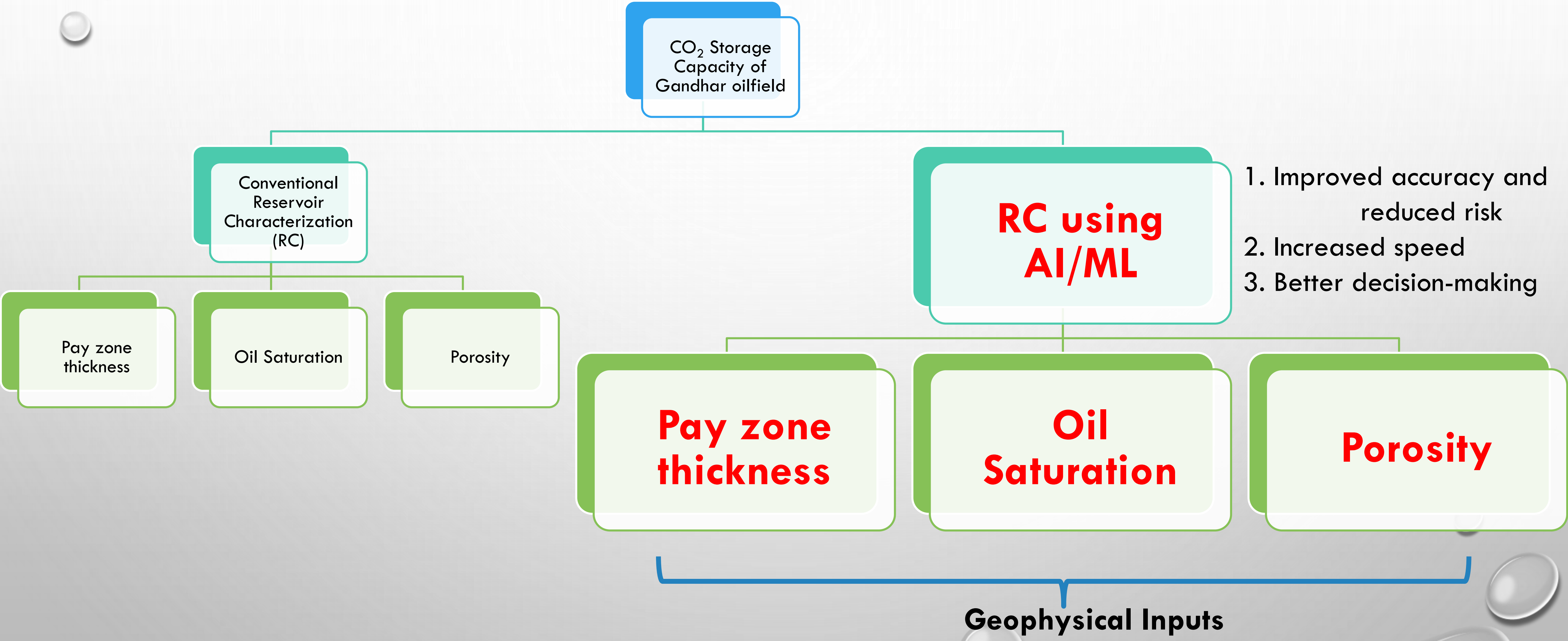

RC using AI/ML

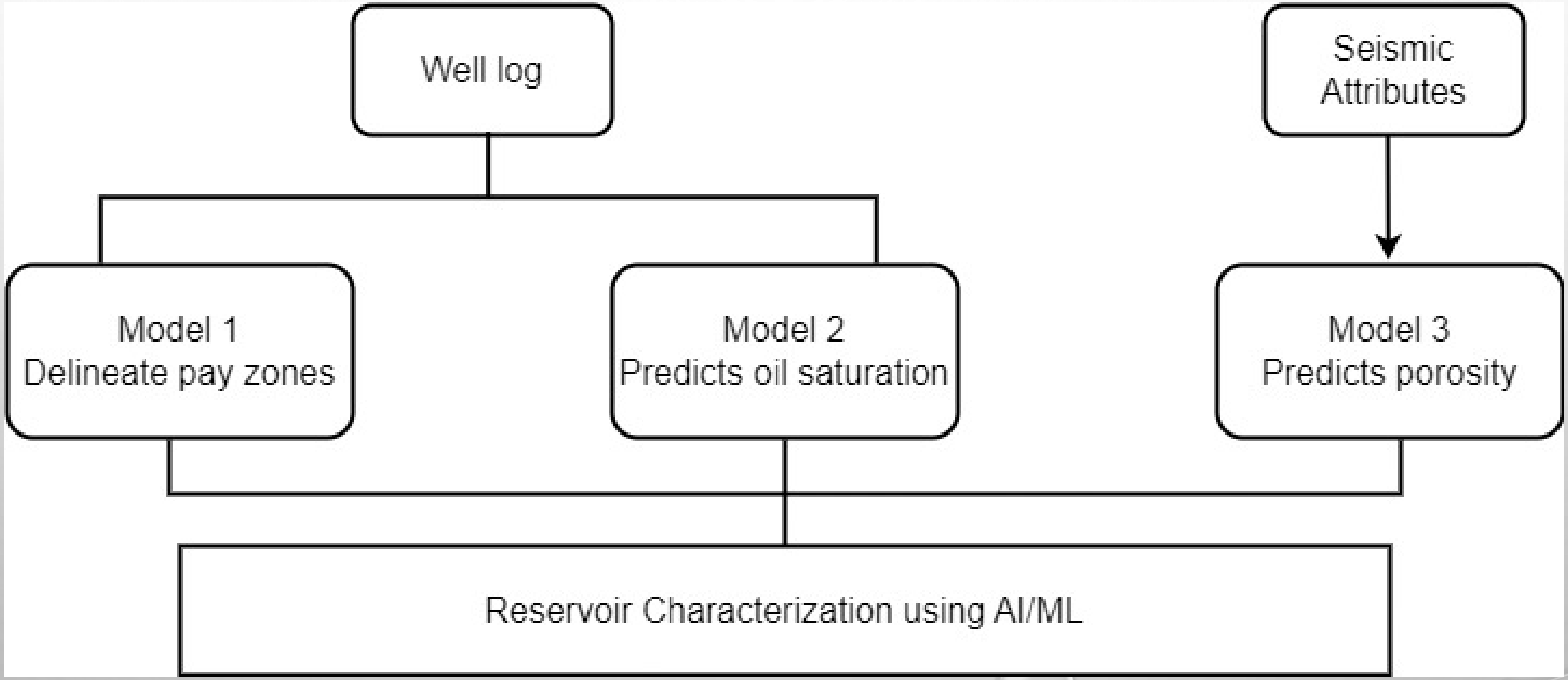

How is a model developed?

Data Preparation

- Clean data, remove outliers, format for processing

Feature Selection

- Using Pearson's correlation

$$r = \frac{\Sigma(x_i - \bar{x})(y_i - \bar{y})}{\sqrt{\Sigma(x_i - \bar{x})^2 \Sigma(y_i - \bar{y})^2}}$$

where, x_i = values of the x-variable in a sample
$\bar{x}$ = mean of the values of the x-variable
y_i = values of the y-variable in a sample
$\bar{y}$ = mean of the values of the y-variable

Algorithm Selection

- Evaluate accuracy or R^2 to select the best algorithm

$$R^2 = 1 - \frac{RSS}{TSS}$$

Validation

- Using blind well prediction

Model 1
Delineates pay zones (sand) using well data

Feature Selection

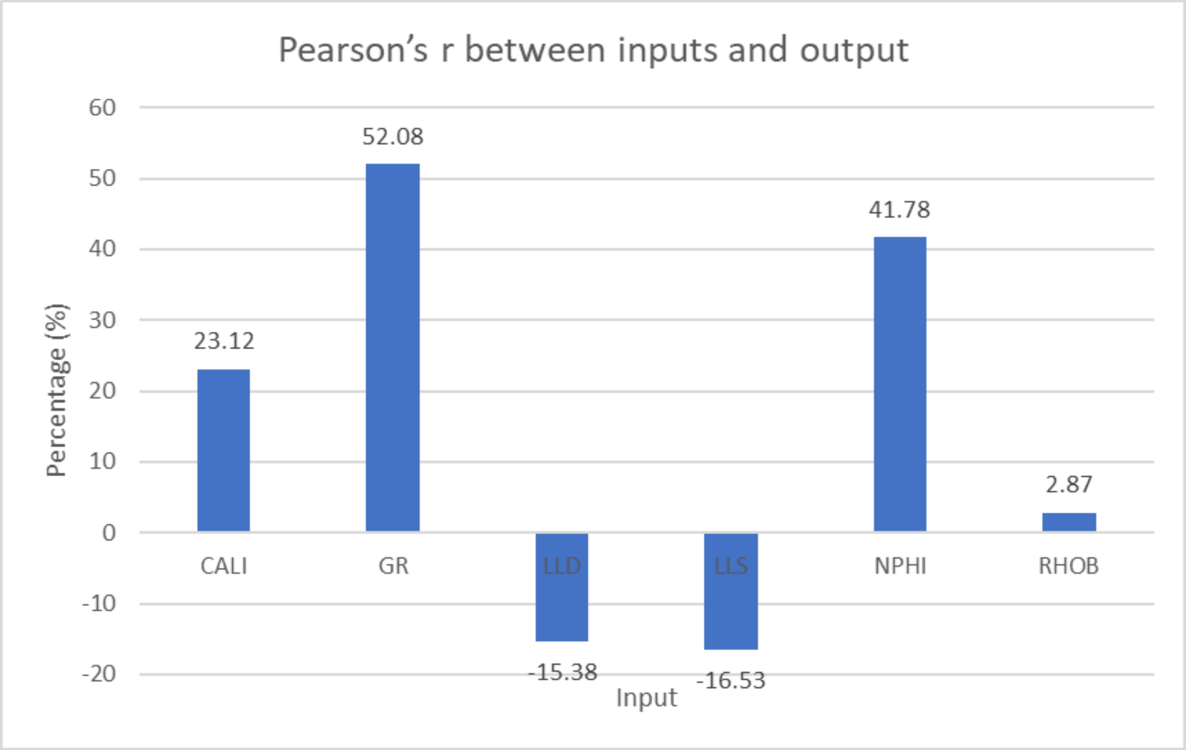

Model Selection

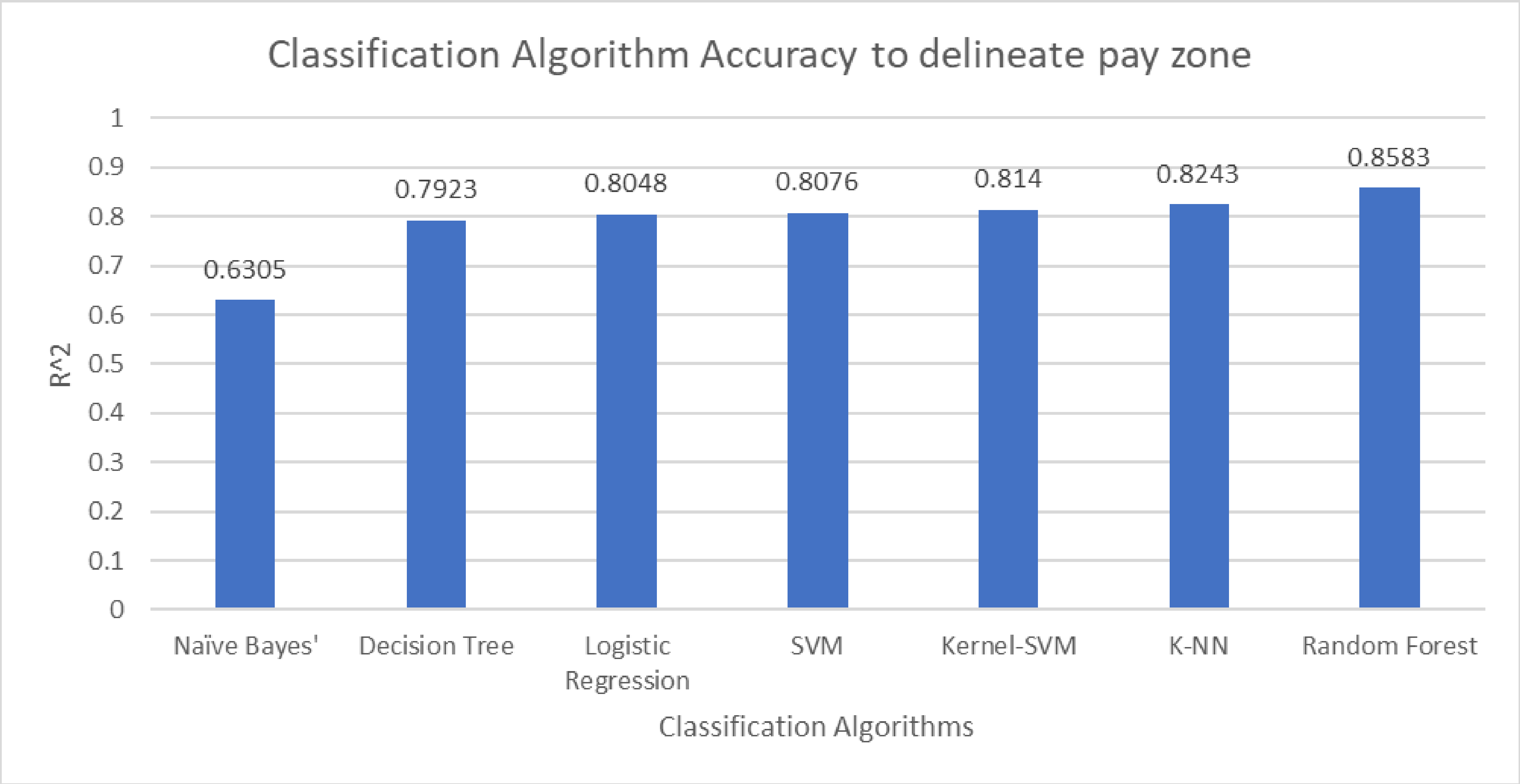

Model Evaluation

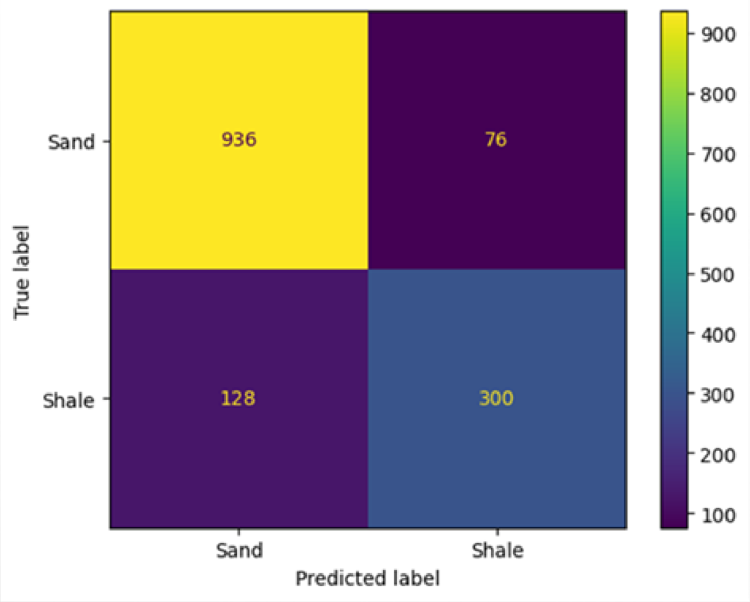

Testing Results

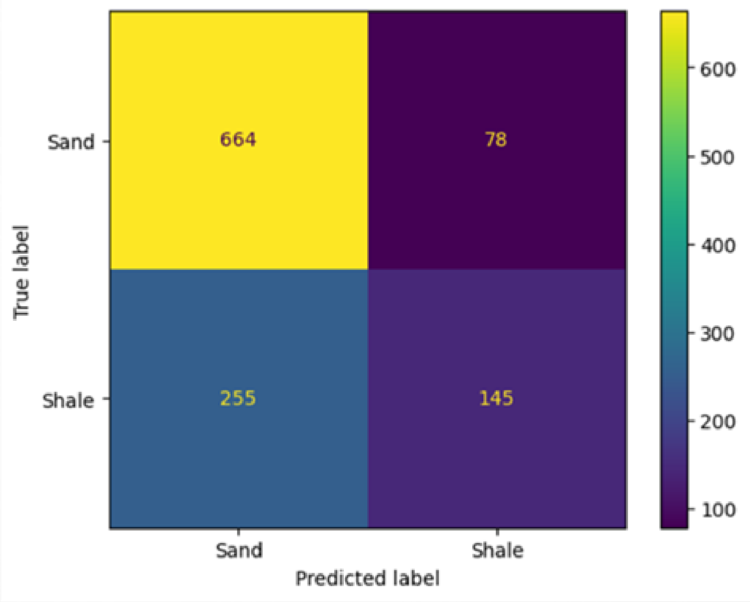

Validation Results

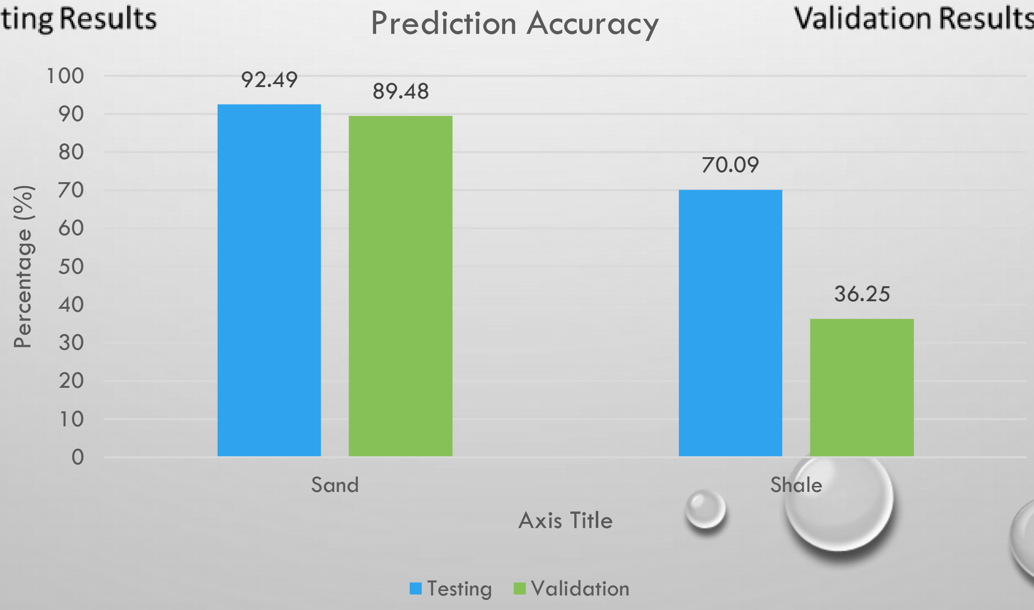

More data = Better results

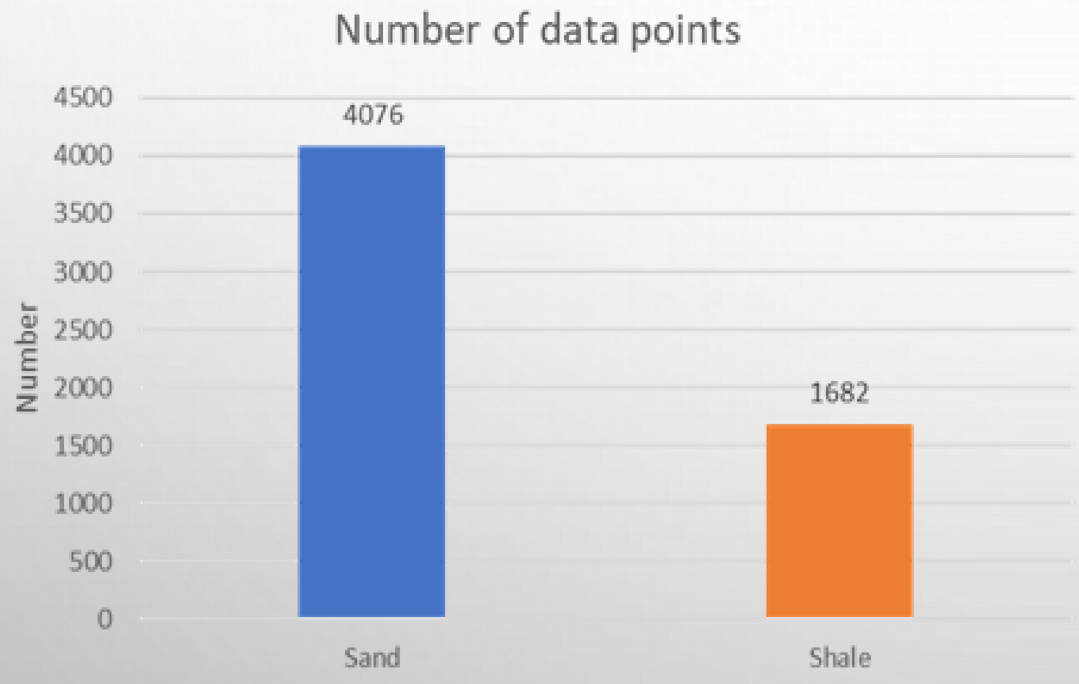

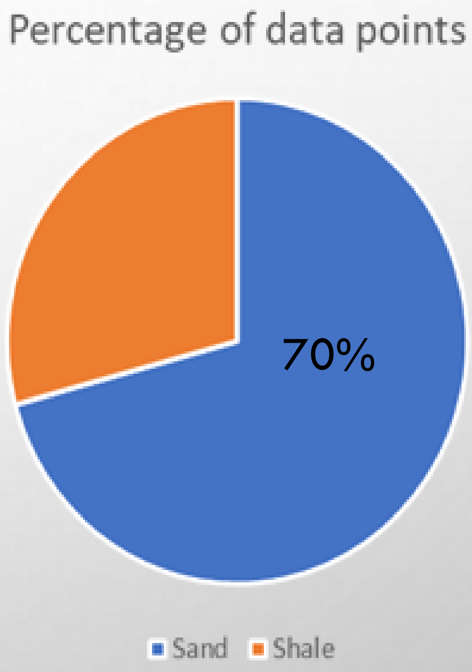

Results

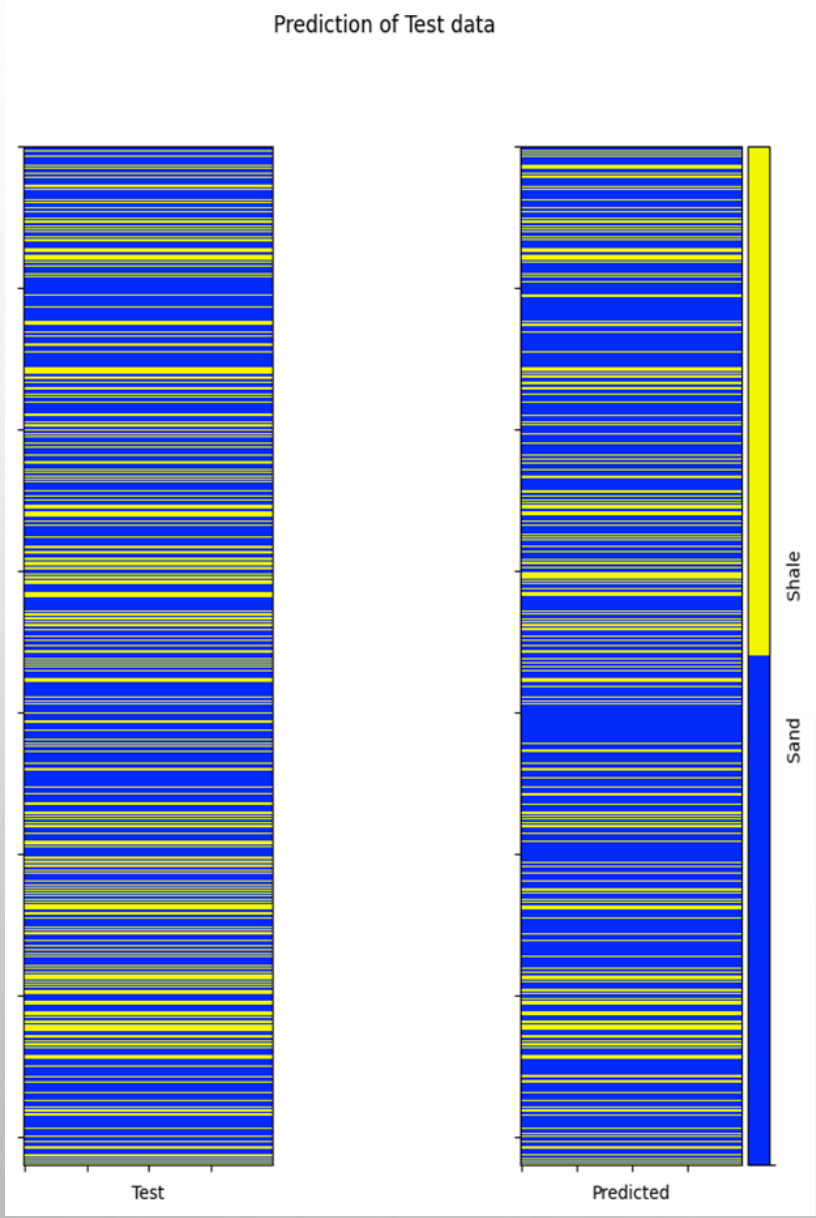

Prediction of Test data
Test
Predicted
Shale
Sand

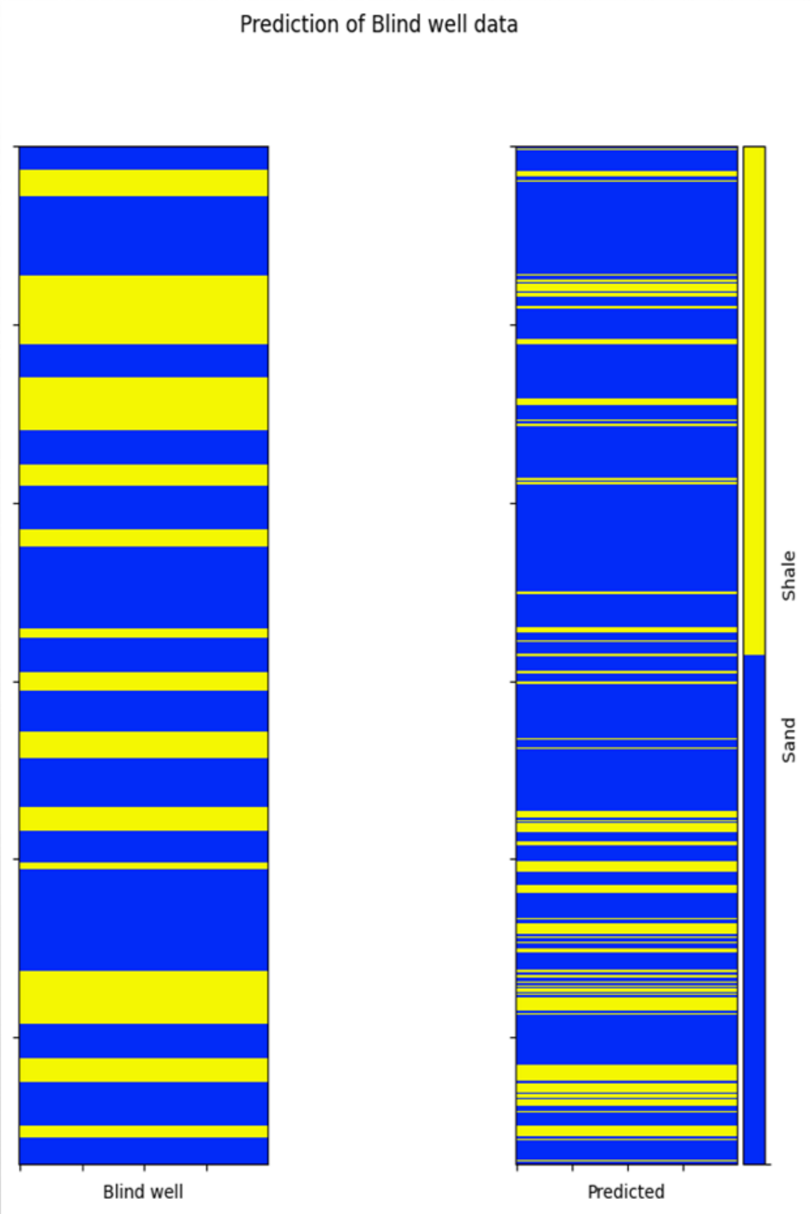

Prediction of Blind well data
Blind well
Predicted
Shale
Sand

Model 2
Predicts oil saturation using well data

Model Selection

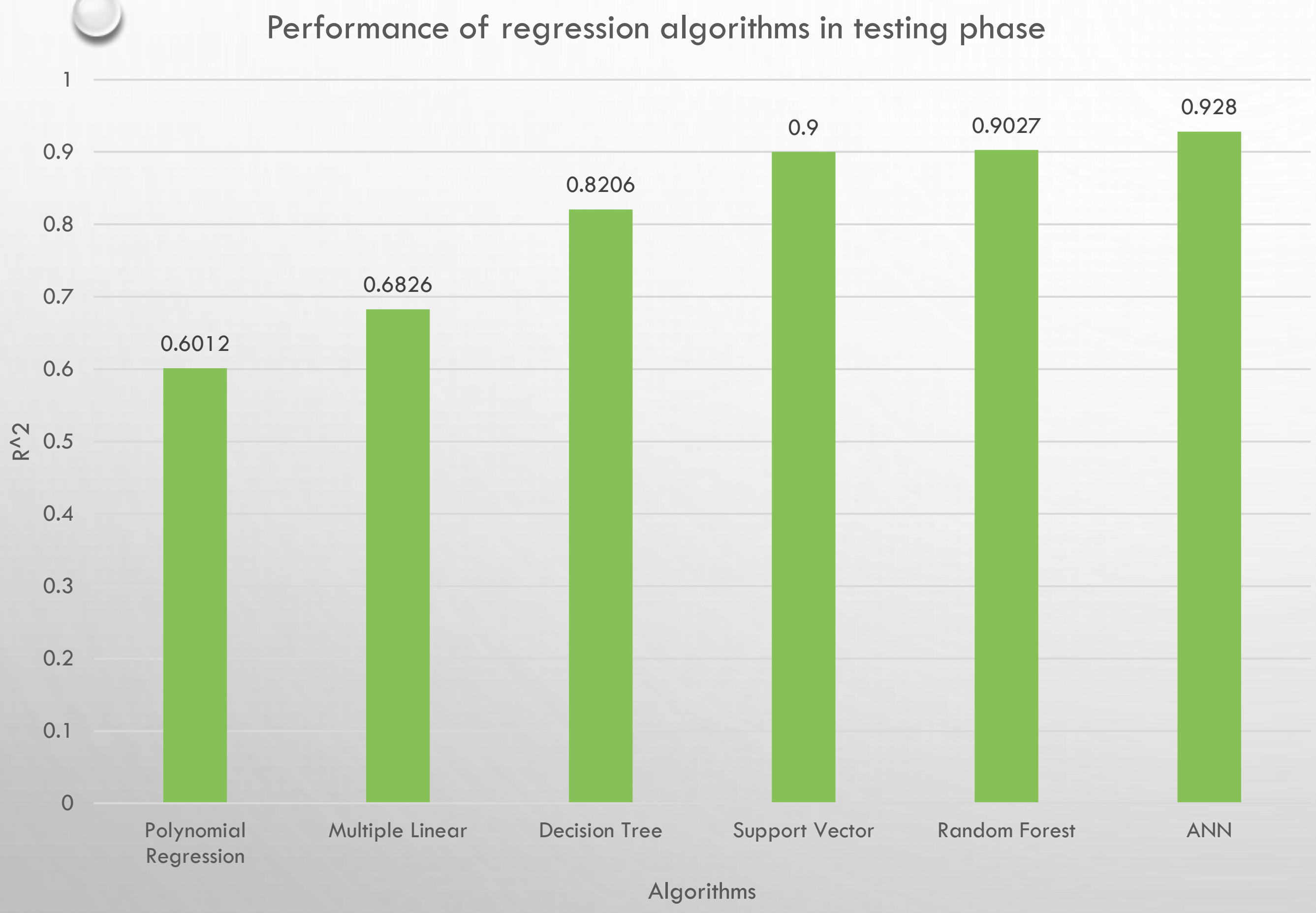

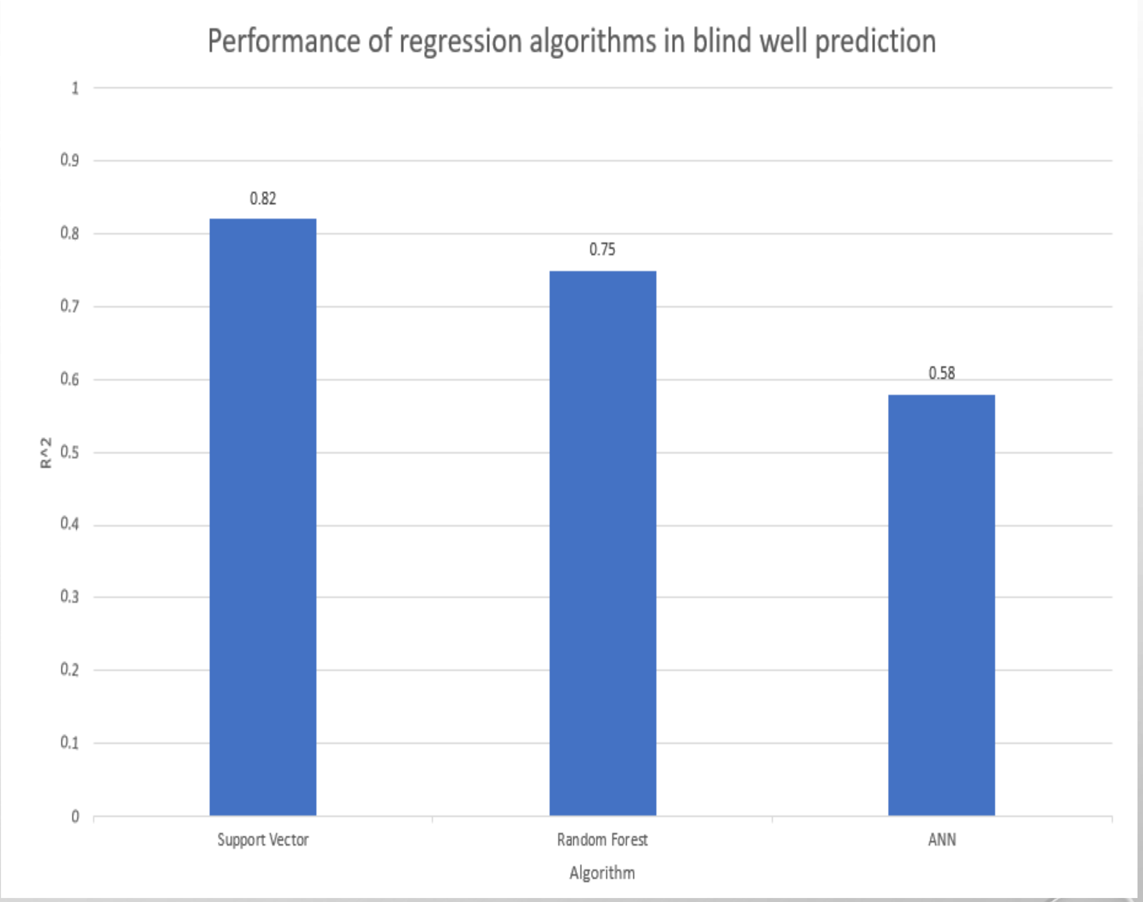

Results

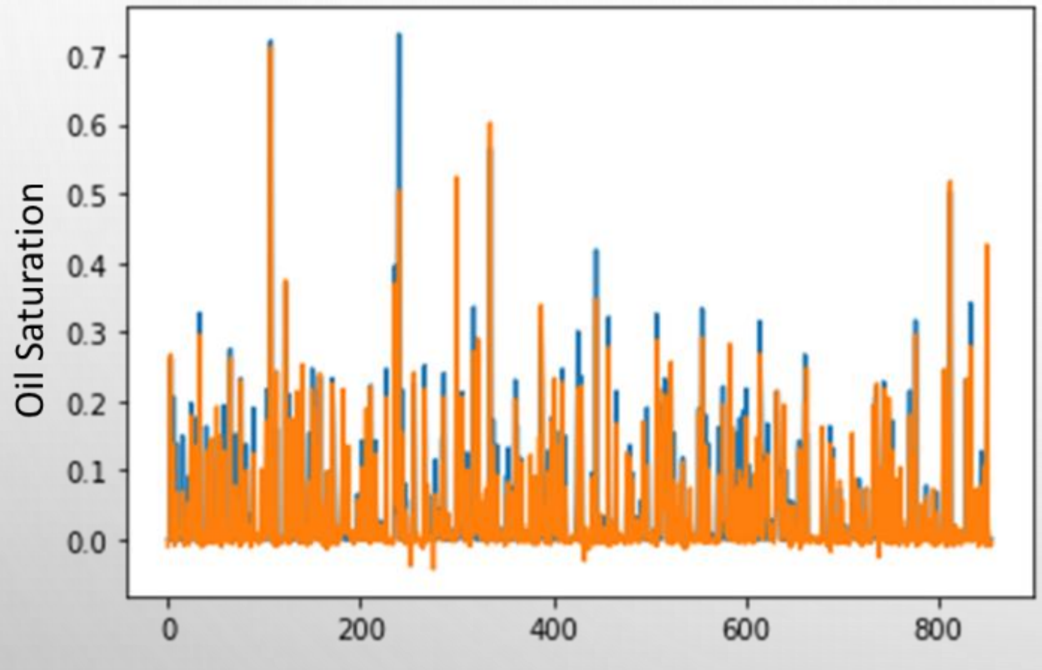

Testing Results

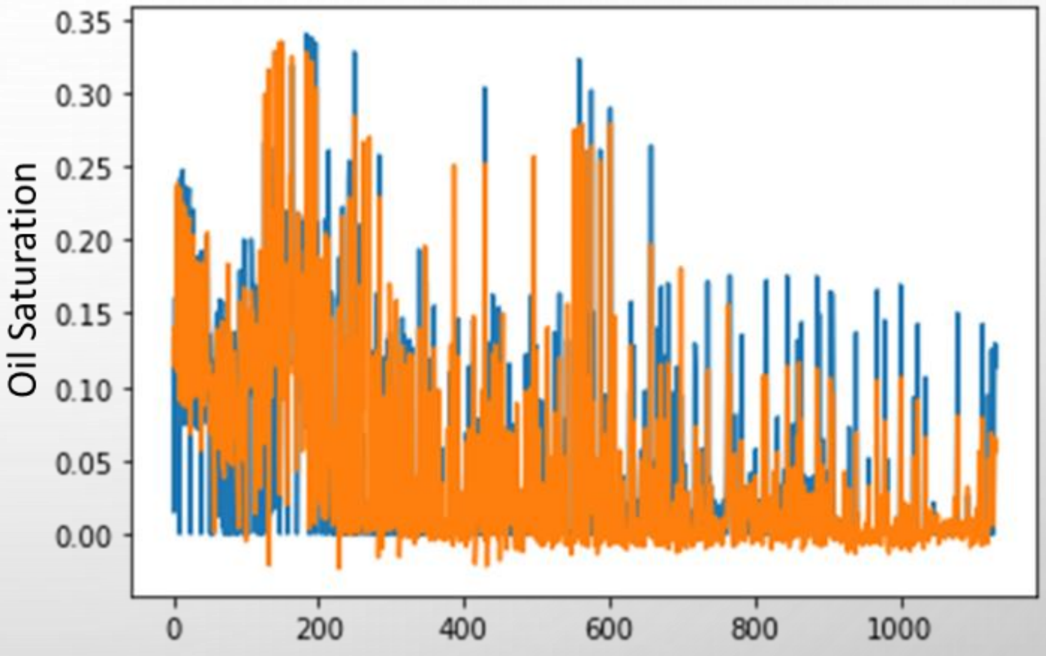

Validation Results

Actual

Predicted

Model 3
Predicts porosity using seismic attributes

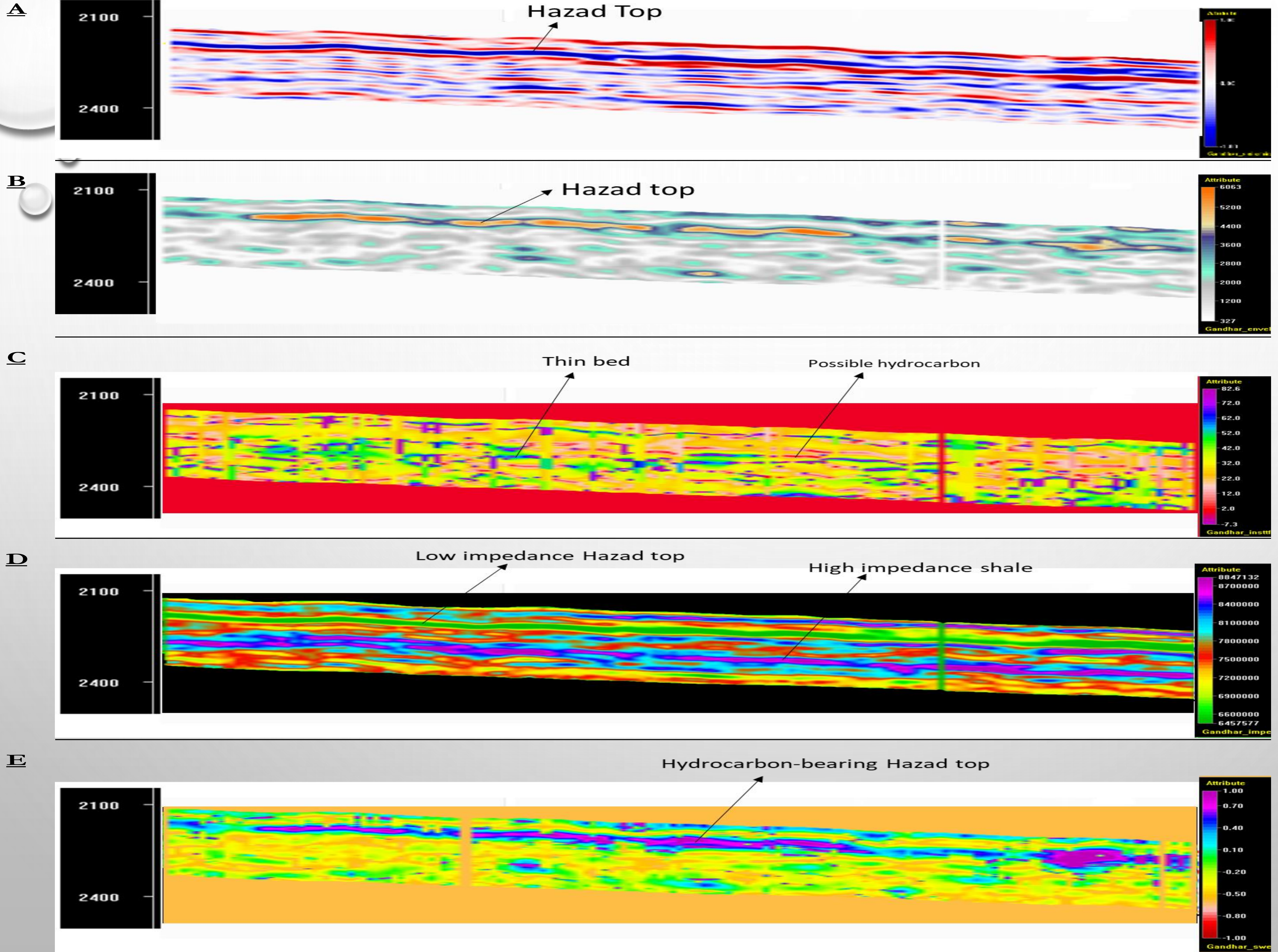

TWT section

Envelope

Instantaneous frequency

Impedance

Sweetness

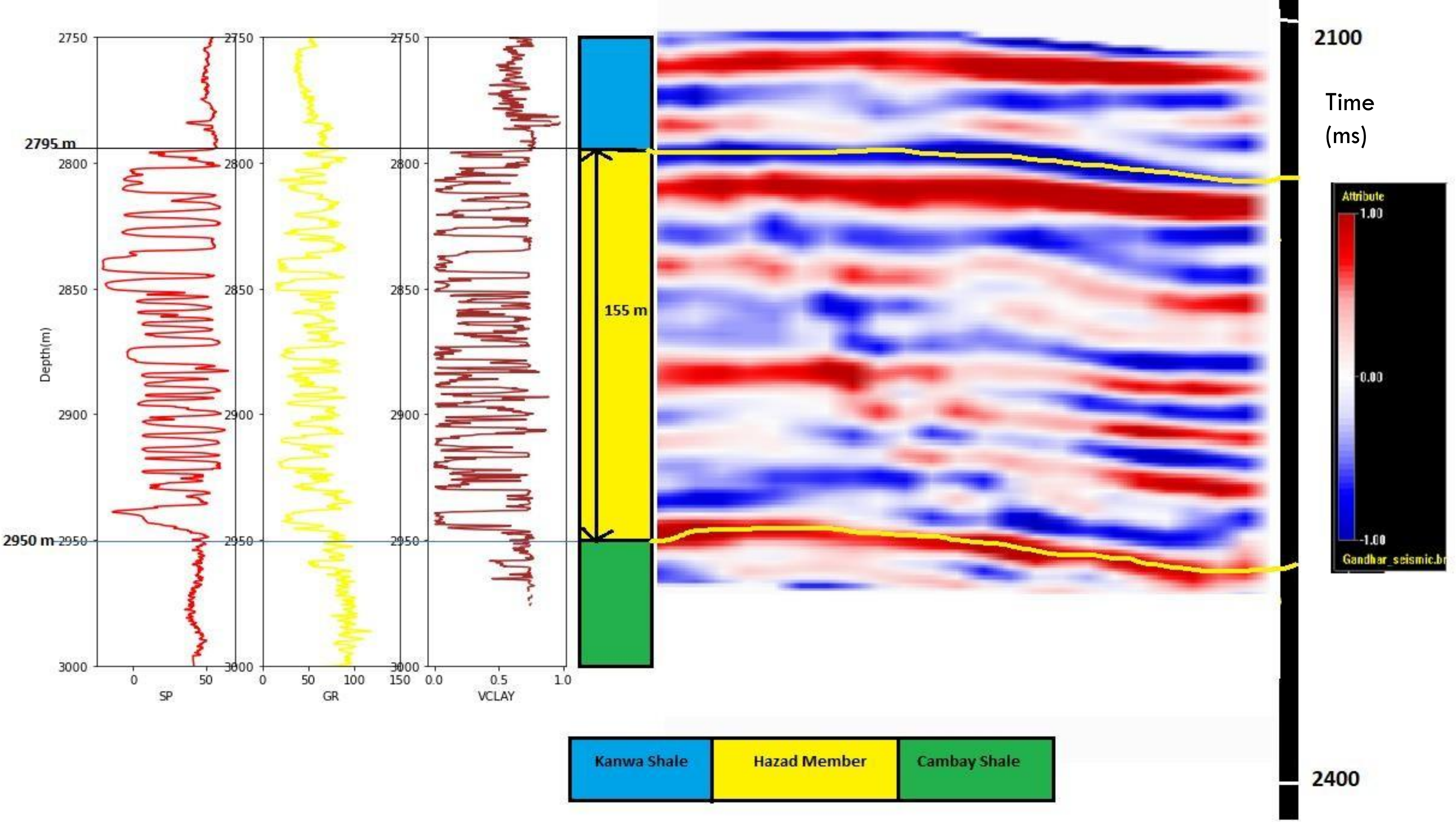
2750
2795 m
2800
2850
2900
2950 m
3000
Depth(m)
0
50
SP
0
50
100
150
GR
0.0
0.5
1.0
VCLAY
155 m
2100
Time
(ms)
2400
Attribute
1.00
0.00
-1.00
Kanwa Shale
Hazad Member
Cambay Shale

Model Selection and Validation

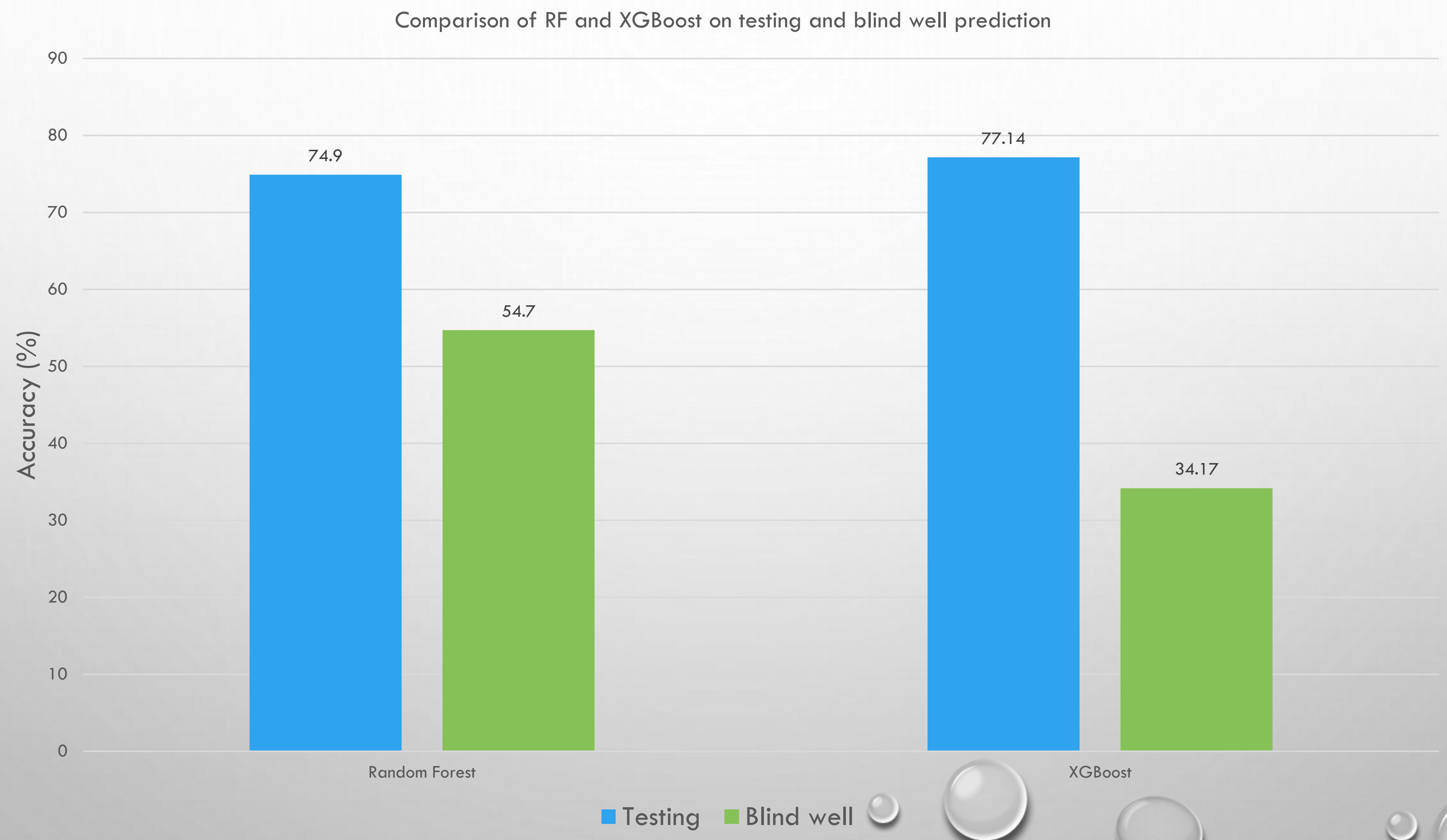

Objectives

CO_2 Storage Capacity of Gandhar oilfield

- Conventional Reservoir Characterization (RC)
  - Pay zone thickness
  - Oil Saturation
  - Porosity
- RC using AI/ML
  - Pay zone thickness
  - Oil Saturation
  - Porosity

Capacity Calculation for CO_2 Storage

$$M_{CO_2} = \rho_{CO_2res}\left[R_f \times A \times h \times \phi \times (1 - S_w) - V_{iw} + V_{pw}\right]$$

ρ_{CO_2res} is the density of CO2 at reservoir conditions

R_f is the recovery factor

A is the area of the field,

h is the effective thickness of the reservoir

ϕ is the porosity,

S_w is the water saturation,

V_{iw} is the volume of injected water
V_{pw} is the volume of produced water.

$$\mathrm{M_{CO_2eff}} = 0.5 \times \mathrm{M_{CO_2res}}$$

Results and Discussion

Property	G_130	G_451	G_425	G_239	Mean
Thickness (m)	45.5	99	87.75	105.75	84.5
Porosity (%)	13.44	11.64	11.59	10.93	11.9
Oil Saturation (%)	14.78	6.5	10.51	14.2	11.49
Water Saturation (%)	85.21	93.5	89.49	85.79	88.51

Parameters	$\rho_{CO_2 res}$	R_f	A	h	ϕ	$S_o = 1 - S_w$	$M_{CO_2 res}$
Units	kg/m3	Fraction	m2	m	Fraction	Fraction	kg
Values	531.75	0.39	5×10^7	84.5	0.119	0.1149	1.198×10^{10}

$$M_{CO_2 res} = 11.98 \text{ MMt}$$

$$M_{CO_2 eff} = 5.99 \text{ Mt} \sim 6 \text{ MMt}$$

Conclusion

Conventional RC used integrated seismic and well-log data to qualitatively interpret the reservoir, identify pay zones, and quantitatively interpret porosity and oil saturation. Visual inspection of well-log data revealed pay zones with an effective thickness of 84.5 m, oil saturation of 11.9%, and porosity of 11.49%.

Three models have been proposed for machine-learning-assisted RC to delineate pay zones, predict oil saturation from well log data, and predict pore class from seismic attributes. Test results determined model selection. Then, a blind well prediction verified the results.

Without field-specific data, a crude storage capacity calculation was shown.

Effective CO_2 storage capacity is 5.99 MMt, while theoretical capacity is 11.98 MMt.

High-porosity and low-permeability pay zones throughout the depleted oil and gas reservoirs of India's Cambay Basin and other sedimentary basins make CO_2 sequestration promising.

This study can be used in other depleted oil and gas fields to find suitable CO_2 injection sites and optimize the injection strategy for safe and effective subsurface CO_2 storage.

Selective References

- Bachu, S., & Shaw, J. (2003). Evaluation of the CO_2 Sequestration Capacity in Alberta's Oil and Gas Reservoirs at Depletion and the Effect of Underlying Aquifers. *J Can Pet Technol 42*.
- Chaki, S., Routray, A., & Mohanty, W. K. (2015). A novel preprocessing scheme to improve the prediction of sand fraction from seismic attributes using neural networks. *IEEE Journal of Selected Topics in Applied Earth Observations and Remote Sensing*, *8*(4), 1808–1820. https://doi.org/10.1109/JSTARS.2015.2404808
- Chopra, S., & Marfurt, K. J. (2007). *SEISMIC ATTRIBUTES FOR PROSPECT IDENTIFICATION AND RESERVOIR CHARACTERIZATION.*
- MOP&NG. (2022). *Draft 2030 Roadmap for Carbon Capture Utilization and Storage (CCUS) for Upstream E&P Companies.*
- Pal, M. (2005). Random forest classifier for remote sensing classification. *International Journal of Remote Sensing*, *26*(1), 217–222. https://doi.org/10.1080/01431160412331269698
- Steyn, M., Oglesby, J., Turan, G., Zapantis, A., Gebremedhin, R., Al Amer, N., Havercroft, I., Ivory-Moore, R., Yang, X., Abu Zahra, M., Pinto, E., Rassool, D., Williams, E., Consoli, C., & Minervini, J. (2022). *GLOBAL STATUS OF CCS 2022.*
- Verma, A. K., Chaki, S., Routray, A., Mohanty, W. K., & Jenamani, M. (2014). Quantification of sand fraction from seismic attributes using Neuro-Fuzzy approach. *Journal of Applied Geophysics*, *111*, 141–155. https://doi.org/10.1016/j.jappgeo.2014.10.005
- Vishal, V., Verma, Y., Chandra, D., & Ashok, D. (2021). A systematic capacity assessment and classification of geologic CO2 storage systems in India. *International Journal of Greenhouse Gas Control*, *111*. https://doi.org/10.1016/j.ijggc.2021.103458


THANK YOU

Supplementary Slides

Future Scope

Multicomponent seismic and time-lapse seismic can add reservoir property and dynamics information. Integrating production, geochemical, and other data can reveal reservoir behaviour and properties.

Detailed pay zone permeability studies can optimise injection strategy.

Tuning hyperparameters is essential for model accuracy and generalization. Evolutionary algorithms tune hyperparameters.

More well data improves algorithm performance.

Regularize the predicting and predictor variables using Empirical Mode Decomposition or Entropy-based Fourier Transform during non-linear mapping, as in Model-3. Information filtering matches the frequencies of both variables and improves mapping accuracy.

A 3D geocellular model of the properties can be created for visualization.

Delineating pay zones using well-logs

Sand	**Shale**
Low GR	High GR
High deflection in SP	Low deflection in SP
High V_p	Low V_p
Low V_{clay}	High V_{clay}

Porosity from well-logs

Neutron Porosity, ϕ_N

Density Porosity, ϕ_D

Total Porosity, $\phi_T = \frac{\phi_N + \phi_D}{2}$

Oil Saturation from well-logs

R_w , R_t

$$S_w = \left(\frac{a}{\phi^m}\frac{R_w}{R_t}\right)^{1/n}$$

$S_o = 1 - S_w$

Inputs

(Archie's Law)

Output

RC using seismic data

TWT section

- Changes in acoustic impedance
- Changes in lithology

Envelope

- $E(t) = \sqrt{T^2(t) + H^2(t)}$
- Shows discontinuities, lithology changes, faults, deposition changes, tuning effects, and SB.

Instantaneous frequency

- $F(t) = \dfrac{d\left(\tan^{-1}\left(\frac{H(t)}{T(t)}\right)\right)}{dt}$
- A low-frequency anomaly is a hydrocarbon indicator.

Impedance

- $\mathrm{Z} = \rho\, V$
- It reveals discontinuities and improves structural delineation. High contrast indicates possible SB and shows unconformities.

Sweetness

- $s(t) = \dfrac{E(t)}{\sqrt{F(t)}}$
- The high sweetness regions in the seismic indicates the presence of hydrocarbon-bearing sand units.

Discussion

❖ **Conventional RC allows for flexibility** in the interpretation of data, enabling geoscientists to adjust the models based on their expertise and intuition.

❖

Advantages of AI/ML in RC	**Disadvantages of AI/ML in RC**
Improved accuracy and reduced risk	High data requirements
Increased speed	Lack of transparency
Better decision-making	Limited understanding of underlying physics

❖ **Random Forest** works well in geophysics:

1. Ability to handle complex datasets
2. Robustness to noise
3. Deals well with non-linear relationships
4. Ability to work with small datasets

❖ **SVR** works well in geophysics because:

1. Deals well with non-linear relationships
2. Can handle a large number of variables

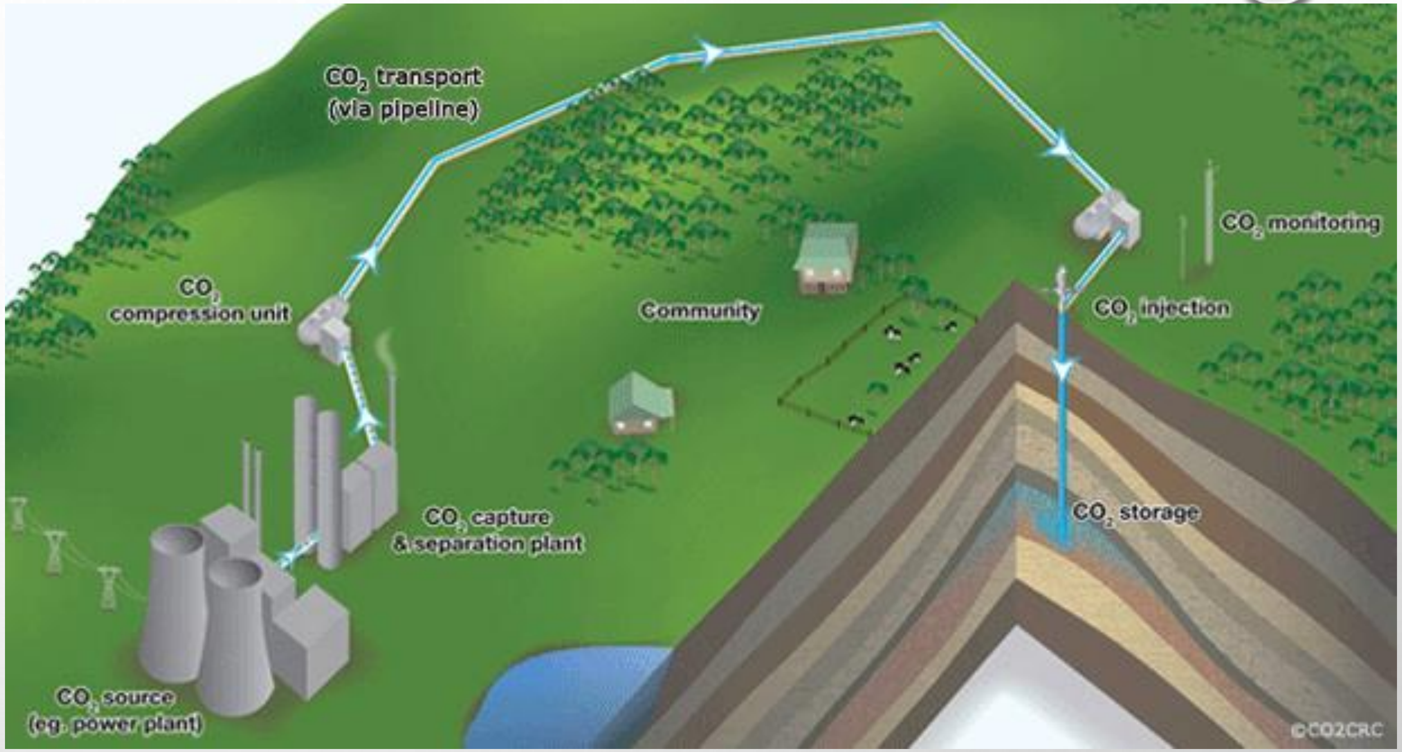

Capture and Store

The Solution: Carbon Capture, Utilization, and Storage (CCUS)

Feature Selection

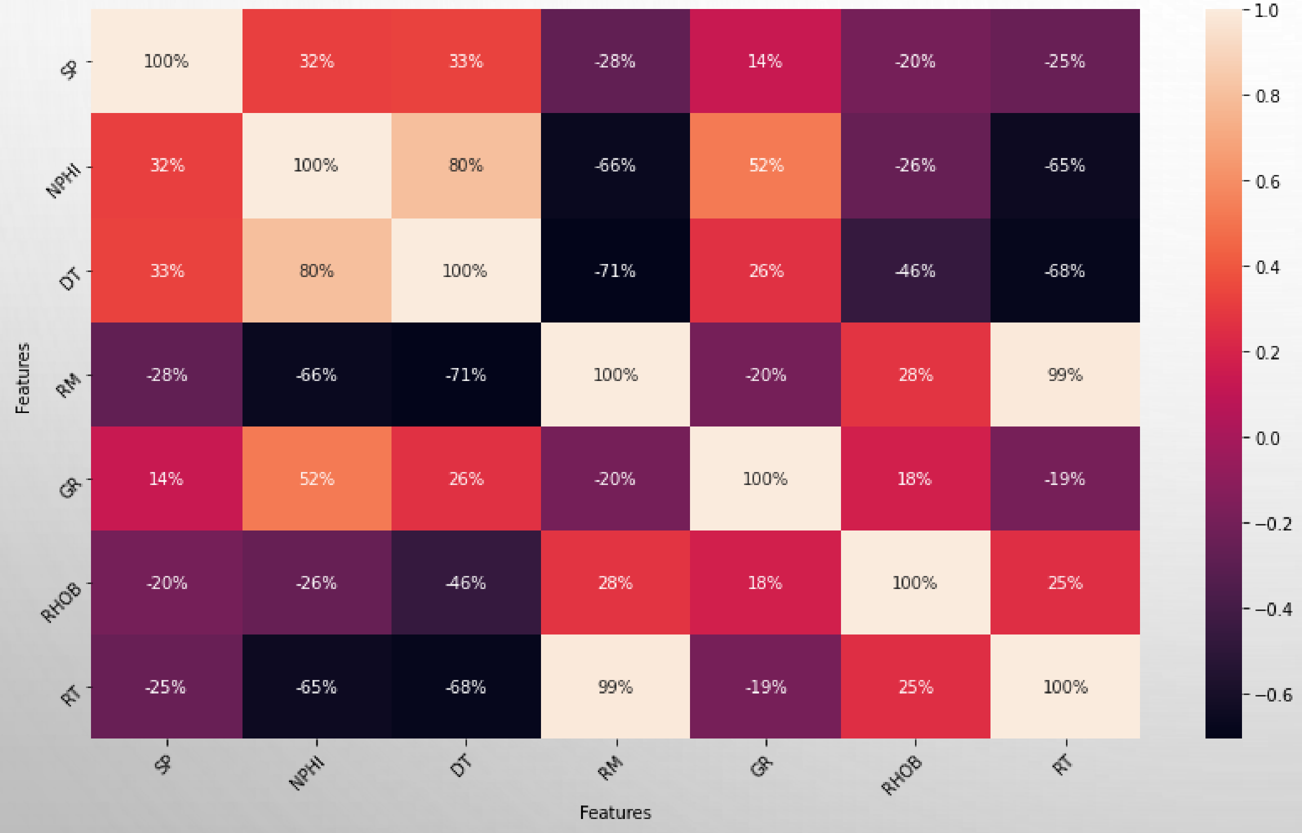

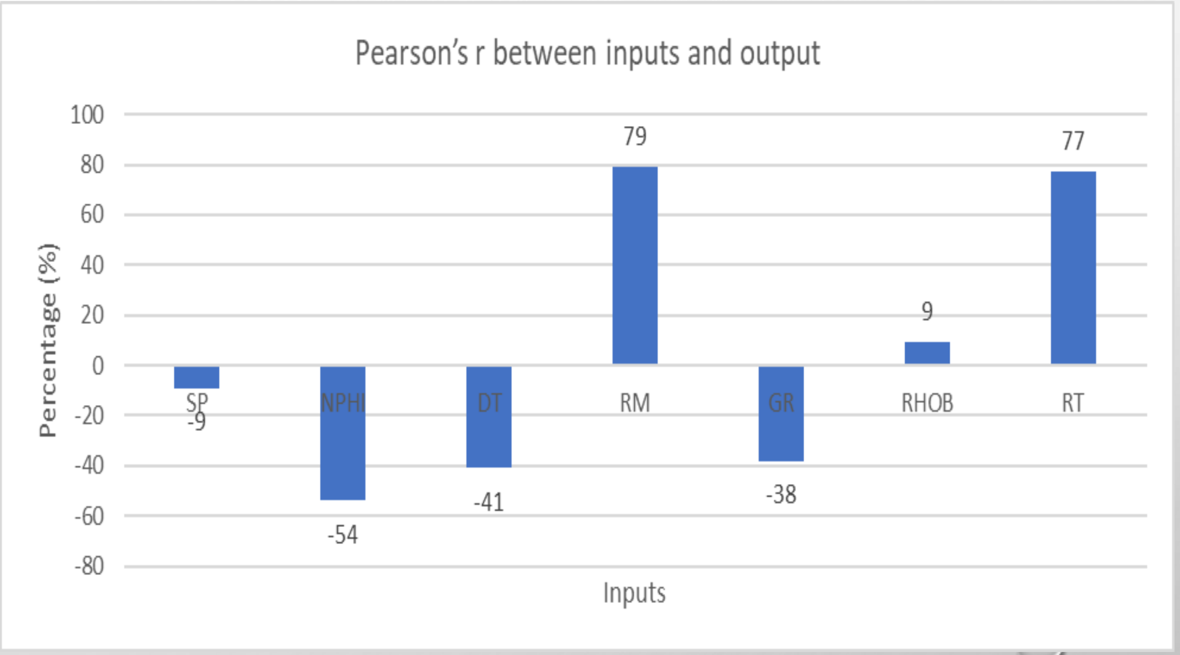

Feature Selection

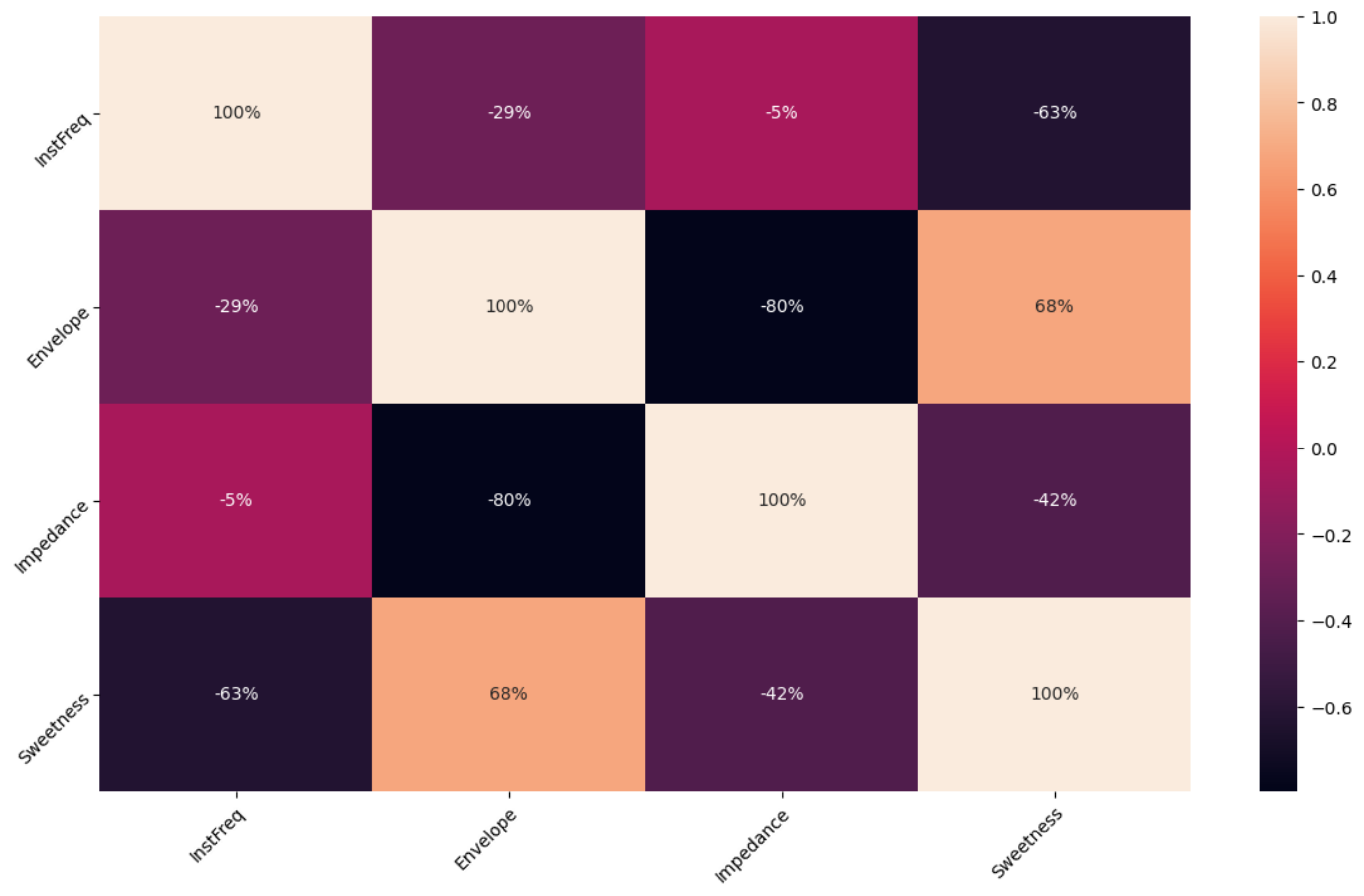

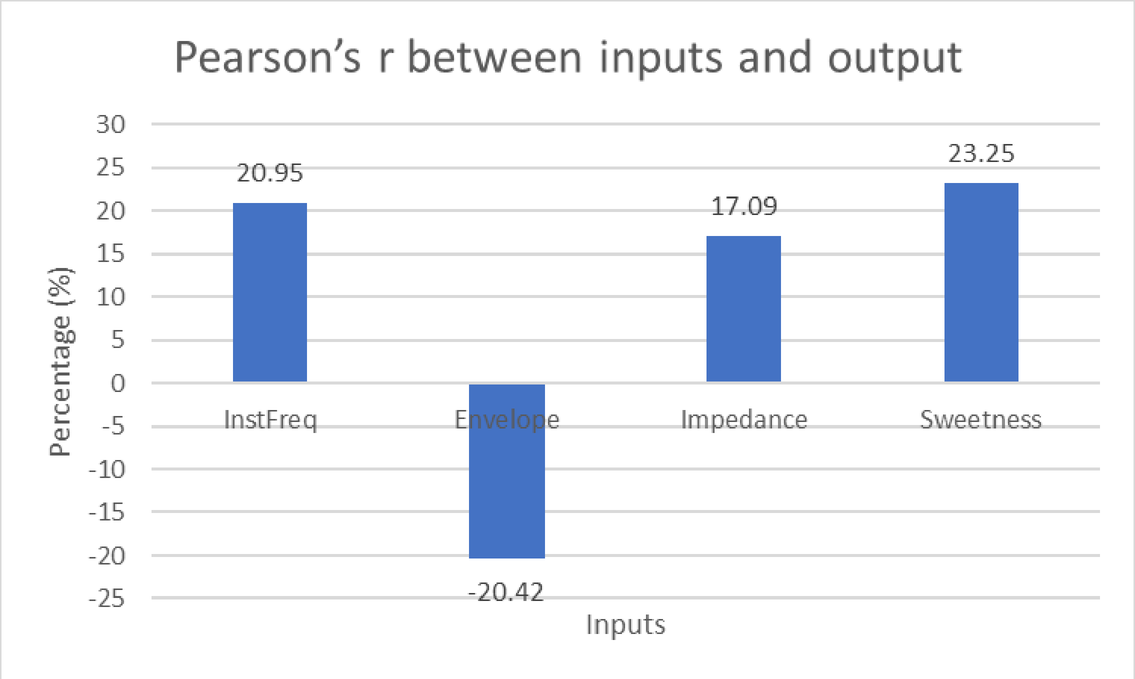

Earth is a ticking bomb!

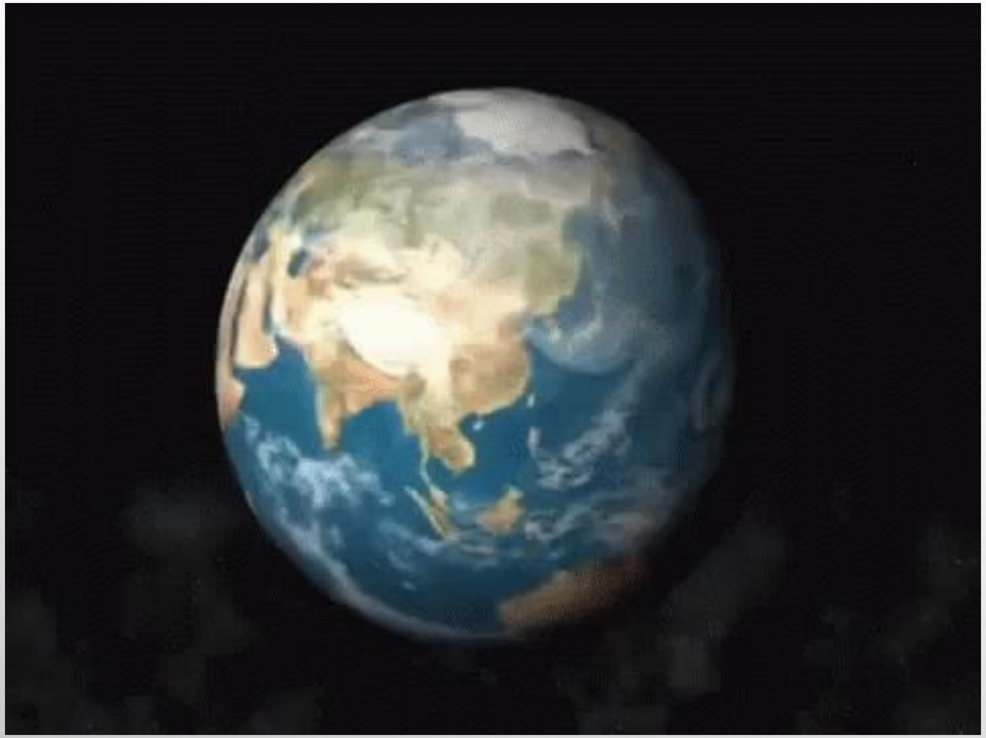

CCUS is the need of the hour!

Geophysicists are the 'Doctors of Mother Earth'!

Role of Geophysics in CCUS

Site Selection	• Seismic reflection surveys identify the thickness and geometry of the storage formation. • Gravity and magnetic surveys can provide information on the structure and composition of the underlying rock formations.
Reservoir characterization	• Porosity and permeability obtained from well-logs and seismic data. • Techniques like seismic tomography, resistivity imaging, and magnetotelluric surveys can provide detailed subsurface images.
Injection monitoring	• Seismic monitoring can detect the movement of the CO_2 plume and any changes in the subsurface • EM surveys can detect changes in the electrical conductivity of the formation.
Post-injection monitoring	• Seismic surveys can detect any changes in the subsurface, such as the movement of the CO2 plume or the development of microseismicity. • Electromagnetic surveys can detect changes in the electrical conductivity of the formation, which can indicate the presence of CO_2.

Dip and Spatial Coverage

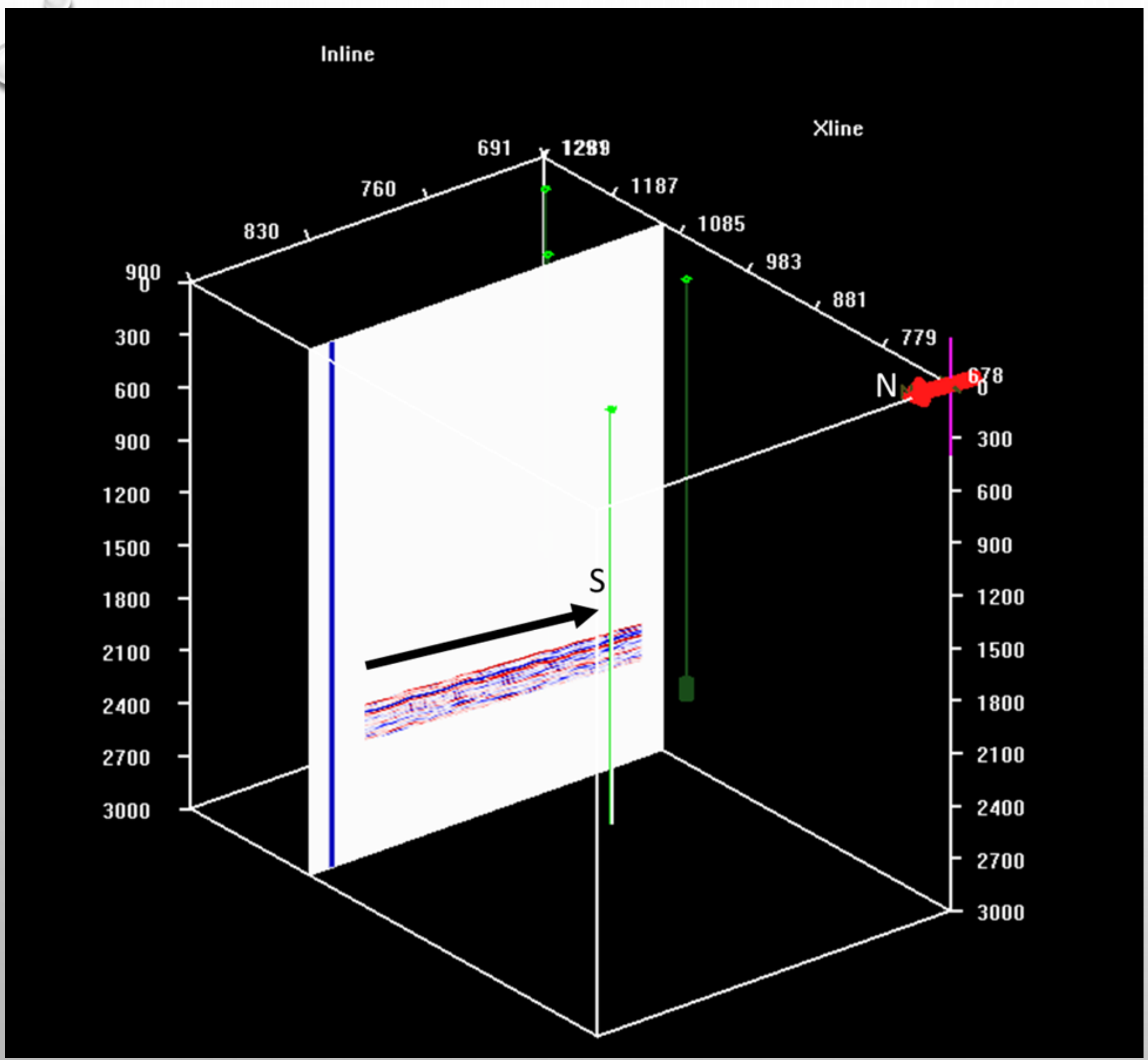

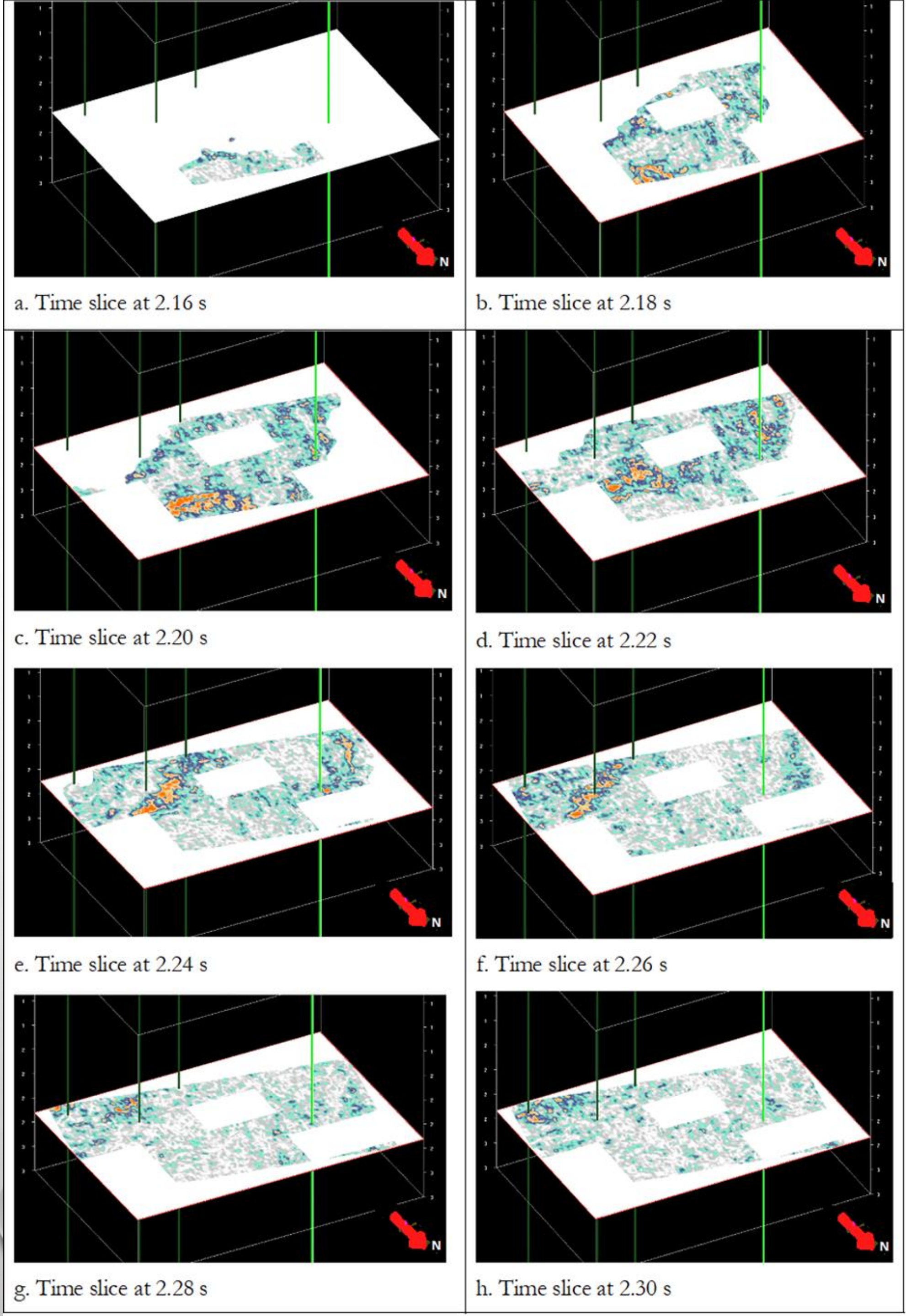
a. Time slice at 2.16 s
b. Time slice at 2.18 s
c. Time slice at 2.20 s
d. Time slice at 2.22 s
e. Time slice at 2.24 s
f. Time slice at 2.26 s
g. Time slice at 2.28 s
h. Time slice at 2.30 s